# Nonlinear Analysis

## Real World Applications

### An International Multidisciplinary Journal
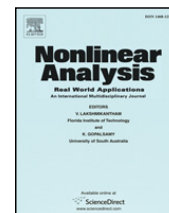
# An alternative characterization of bit-sticking phenomena in a multi-degree-of-freedom controlled drillstring

Eva M. Navarro-López *

*School of Computer Science, Centre for Interdisciplinary Computational and Dynamical Analysis, The University of Manchester, Oxford Road, Kilburn Building, Manchester, M13 9PL, United Kingdom*

## A R T I C L E   I N F O

## A B S T R A C T

A piecewise-smooth model of three degrees of freedom, which exhibits friction-induced stick-slip oscillations, is considered. This model corresponds to a simplified torsional lumped-parameter model of an oilwell drillstring. An alternative method to characterize the stick-slip motion and other bit-sticking problems in such a drilling system is proposed. This method is based on the study of the relationships between the different types of system equilibria and the existing sliding motion when the bit velocity is zero. It is shown that such a sliding motion plays a key role in the presence of nondesired bit oscillations and transitions. Furthermore, a proportional-integral-type controller is designed in order to drive the rotary velocities to a desired value. The ranges of the controller and the system parameters which lead to a closed-loop system without bit-sticking phenomena are identified.

© 2008 Elsevier Ltd. All rights reserved.

## 1. Introduction

Discontinuous elements define the behaviour of dynamical systems in different areas of Science and Engineering; for instance, mechanical systems with friction, impacts, electronic power converters, or systems with sudden state changes. Discontinuous dynamical systems present a wide variety of standard and nonstandard bifurcations. Due to this fact, the analysis of nondesired transitions and bifurcations is a key issue in order to ensure good performance and quality in the control design [1–3].

The bifurcation analysis of mechanical systems with friction-induced self-excited stick-slip oscillations has attracted the attention of researchers in the last two decades [4–9]. These works usually treat systems of two degrees of freedom (DOF). In addition, the existence of stick-slip periodic motion is studied from different viewpoints. In this paper, a 3-DOF lumped-parameter piecewise-smooth (PWS) model is considered. It is the torsional model of a simplified conventional vertical oilwell drillstring. This model is a particular case of the generic *n*-DOF model proposed in [10], and considers the drill pipe dynamics. It is more general than the torsional lumped-parameter models of one and two DOF previously proposed [11–19].

Oilwell drillstrings exhibit a wide variety of complex phenomena and nondesired oscillations due to the presence of different types of friction. These oscillations are a source of component failures, which reduce penetration rates and increase drilling operation costs [13,17,19]. Special attention is paid to the effects of bit-rock friction and torsional mechanical vibrations, mainly, stick-slip oscillations appearing at the bottom-hole assembly (BHA) and other bit-sticking phenomena which cause the bit to remain motionless. Different control schemes have been proposed in order to suppress drillstring stick-slip oscillations. For example, [11,14,20] proposed a vibration absorber at the top of the drillstring. A classical PID
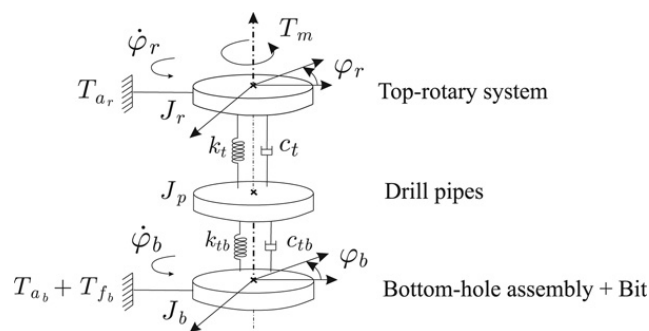
---

**Fig. 1.** Mechanical model describing the torsional behaviour of a simplified drillstring.

control structure at the surface is used in [15,19,21]. More sophisticated techniques are used in [17,16] where a linear quadratic regulator and a linear $H^\infty$ control are used, respectively. In most of these works, no bifurcation analysis of the system and the controller parameters is made, and the influence of the weight on the bit (WOB) is not analysed. The importance of the WOB in drillstring dynamical behaviour was established previously in [22].

In this paper, following the results given in [10], an alternative method for analysing bit stick-slip oscillations and other bit transitions is given. A sliding motion arises when the bit velocity is zero, and it is the main cause of bit stick-slip oscillations and the permanent stuck bit. Such a sliding motion depends mainly on the WOB, the rotary speed at the top-rotary system and the torque applied by the surface motor. Moreover, a linear proportional-integral (PI) action controller is designed in the paper. The controller parameters are chosen so that nondesired system transitions cannot appear. The relationships between the sliding motion and the different types of system equilibria are established for the open and closed-loop system configurations.

The model and the controller structure were proposed in [23], however, in this paper, the analysis of the open-loop and the closed-loop systems is extended.

The proposed controller has to be interpreted as an off-line safe-parameter selection method. The complexity of oilwell drillstrings and drilling practices makes unfeasible the use of an automatic controlled system. The model and controller proposed can help the driller to design, before starting the operation, the well drilling profile with reference values for the torque at the top-rotary system ($u$), the WOB and desired rotary velocities ($\Omega$). For a combination of ($W_{ob}$, $\Omega$), the torque $u$ would be calculated in order to avoid nondesired bit phenomena.

## 2. A torsional discontinuous model of the drillstring

Three main parts of a conventional vertical oilwell drillstring are considered: (1) the rotating mechanism at the surface, (2) the set of drill pipes which are screwed one to each other to form a long pipeline, (3) the BHA, which consists of the drill collars, the stabilizers, a heavy-weight drill pipe and the bit. The drill collars and pipe sections just above the bit are stiffer than the drill pipes and the bit in order to prevent the drillstring from underbalancing. While the length of the BHA remains constant, the total length of the pipeline increases as the drilling operation makes progress, that is the reason why it is important to separate the drill pipes dynamics from the BHA dynamics. In this paper, the BHA will be also referred to as bit.

Fig. 1 shows a simplified torsional model of a conventional vertical drillstring. $J_r$, $J_p$ and $J_b$ are the inertias of the top-rotary system, the drill pipes and the BHA, respectively. The inertias are connected one to each other by linear springs with torsional stiffness ($k_t$, $k_{tb}$) and torsional damping ($c_t$, $c_{tb}$). A viscous damping torque is considered at the top-drive system ($T_{a_r}$) and at the bit ($T_{a_b}$). A dry friction torque ($T_{f_b}$) is considered at the bit. The equations of motion are:

$$\ddot{\varphi}_r = -\frac{c_t}{J_r}(\dot{\varphi}_r - \dot{\varphi}_p) - \frac{k_t}{J_r}(\varphi_r - \varphi_p) + \frac{T_m - T_{a_r}(\dot{\varphi}_r)}{J_r},$$

$$\ddot{\varphi}_p = \frac{c_t}{J_p}(\dot{\varphi}_r - \dot{\varphi}_p) + \frac{k_t}{J_p}(\varphi_r - \varphi_p) - \frac{c_{tb}}{J_p}(\dot{\varphi}_p - \dot{\varphi}_b) - \frac{k_{tb}}{J_p}(\varphi_p - \varphi_b), \quad (1)$$

$$\ddot{\varphi}_b = \frac{c_{tb}}{J_b}(\dot{\varphi}_p - \dot{\varphi}_b) + \frac{k_{tb}}{J_b}(\varphi_p - \varphi_b) - \frac{T_b(\dot{\varphi}_b)}{J_b},$$

with $\varphi_i$, $\dot{\varphi}_i$ ($i \in \{r, p, b\}$) the angular displacements and the angular velocities of the drillstring elements, respectively. $T_m$ is the torque applied by the electrical motor at the surface. The actuator dynamics is not considered, and $T_m = u$, with $u$ the control input. $T_{a_r} = c_r\dot{\varphi}_r$, with $c_r$ the viscous damping coefficient. The system state vector **x** is defined as:

$$\mathbf{x} = (\dot{\varphi}_r, \varphi_r - \varphi_p, \dot{\varphi}_p, \varphi_p - \varphi_b, \dot{\varphi}_b)^T = (x_1, x_2, x_3, x_4, x_5)^T. \quad (2)$$

Finally, $T_b(x_5) = T_{a_b}(x_5) + T_{f_b}(x_5)$ is the torque on the bit, with $T_{a_b} = c_b x_5$ representing the influence of the mud drilling on the bit behaviour. $T_{f_b}(x_5)$ is the friction modelling the bit-rock contact, which is defined as:

$$T_{f_b}(x_5) = W_{ob} R_b \mu_b(x_5) \text{sign}(x_5), \tag{3}$$

where $W_{ob} > 0$ is the weight on the bit, $R_b > 0$ is the bit radius and $\mu_b(x_5)$ is the bit dry friction coefficient considered as,

$$\mu_b(x_5) = \left[ \mu_{c_b} + (\mu_{s_b} - \mu_{c_b}) \exp^{-\frac{\gamma_b}{v_f}|x_5|} \right], \tag{4}$$

with $\mu_{s_b}, \mu_{c_b} \in (0, 1)$ the static and the Coulomb friction coefficients associated with $J_b$; $0 < \gamma_b < 1$ and $v_f > 0$. In addition, the Coulomb and the static friction torques are $T_{c_b}$ and $T_{s_b}$, respectively, with:

$$T_{c_b} = W_{ob} R_b \mu_{c_b}, \qquad T_{s_b} = W_{ob} R_b \mu_{s_b}. \tag{5}$$

The exponential decaying behaviour of $T_b$ coincides with experimental bit torque values and is inspired in the models given in [13,15,21].

In Eq. (3), the sign function is considered as:

$$\begin{aligned} \text{sign}(x_5) &= x_5/|x_5| &&\text{if } x_5 \neq 0, \\ \text{sign}(x_5) &\in [-1, 1] &&\text{if } x_5 = 0. \end{aligned} \tag{6}$$

Thus, the function $T_{f_b}(x_5)$ has the form:

$$T_{f_b}(x_5) = \begin{cases} T_{f_b}^+(x_5) & \text{if } x_5 > 0, \\ T_{f_b}^-(x_5) & \text{if } x_5 < 0, \end{cases}$$
$$T_{f_b}(x_5) \in \left[ -T_{s_b}, T_{s_b} \right] \quad \text{if } x_5 = 0, \tag{7}$$

with:

$$\begin{aligned} T_{f_b}^+(x_5) &= W_{ob} R_b \left[ \mu_{c_b} + (\mu_{s_b} - \mu_{c_b}) \exp^{-\frac{\gamma_b}{v_f} x_5} \right], \\ T_{f_b}^-(x_5) &= -W_{ob} R_b \left[ \mu_{c_b} + (\mu_{s_b} - \mu_{c_b}) \exp^{\frac{\gamma_b}{v_f} x_5} \right]. \end{aligned} \tag{8}$$

In Section 3, an analysis of the different dynamical behaviours appearing when $x_5 = 0$ will be addressed. For this purpose, an adequate mathematical model on the discontinuity surface $x_5 = 0$ will be chosen.

Using (2), system (1) can be written as:

$$\begin{aligned} \dot{x}_1 &= \frac{1}{J_r} \left[ -(c_t + c_r) x_1 - k_t x_2 + c_t x_3 + u \right], \quad \dot{x}_2 = x_1 - x_3, \\ \dot{x}_3 &= \frac{1}{J_p} \left[ c_t x_1 + k_t x_2 - (c_t + c_{tb}) x_3 - k_{tb} x_4 + c_{tb} x_5 \right], \quad \dot{x}_4 = x_3 - x_5, \\ \dot{x}_5 &= \frac{1}{J_b} \left[ c_{tb} x_3 + k_{tb} x_4 - (c_{tb} + c_b) x_5 - T_{f_b}(x_5) \right]. \end{aligned} \tag{9}$$

or in a compact form,

$$\dot{\mathbf{x}}(t) = \mathbf{A}\mathbf{x}(t) + \mathbf{B}u(t) + \mathbf{T}_f(\mathbf{x}(t)). \tag{10}$$

In the following simulations, the data corresponding to a real drillstring design reported in [24] are used:

$$\begin{aligned} &J_r = 2122 \text{ kg m}^2, J_b = 471.9698 \text{ kg m}^2, J_p = 750 \text{ kg m}^2, \\ &k_t = 698.06314 \text{ N m/rad}, k_{tb} = 907.482089 \text{ N m/rad}, R_b = 0.155575 \text{ m}, \\ &c_t = 139.612629 \text{ N m s/rad}, c_{tb} = 181.49641 \text{ N m s/rad}, \\ &c_r = 425 \text{ N m s/rad}, c_b = 50 \text{ N m s/rad}, \\ &\mu_{c_b} = 0.5 \, \mu_{s_b} = 0.8, D_v = 10^{-6}, \gamma_b = 0.9, v_f = 1. \end{aligned} \tag{11}$$

## 3. Open-loop system dynamical properties: Transitions and bifurcations

Two dynamical properties explain the existence of bit stick-slip oscillations and the permanent stuck bit: (1) the existence of a sliding motion which gives rise to an asymptotically stable quasiequilibrium on the sliding surface, and (2) when

velocities are greater than zero, the existence of a unique standard equilibrium point which can become unstable. These phenomena depend on three key manipulable drilling parameters: (1) the WOB, (2) the steady rotary speed, and (3) the torque applied by the surface motor ($u$). In this section, the two inputs WOB and $u$ will be considered constant.

The features of the open-loop system which will be key in the control design are:

(1) The sticking of the bit can be described by means of the conceptual sliding motion on the surface $x_5 = 0$. This sliding motion has the following characteristics:
   - The dynamics on the sliding surface depends mainly on the parameter $u$.
   - The sliding surface may alternate between being attractive or repulsive.
   - The sliding surface contains an asymptotically stable quasiequilibrium.
   - Different dynamical behaviours appear on the surface of discontinuity depending on the relative position of the quasiequilibrium with respect to the boundary of the sliding region.
   - The sliding surface, its region of attraction and the region of attraction of the quasiequilibrium change provided that some system parameters change.
(2) The stability of the unique standard equilibrium point when $x_5 > 0$ influences the bit behaviour. The desired situation is when this equilibrium is stable, however:
   - The standard equilibrium is locally asymptotically stable depending on the values of $W_{ob}$, the torque $u$ and the rotary velocity at the equilibrium.
   - The loss of stability of the standard equilibrium point is mainly due to the presence of Hopf bifurcations.

### 3.1. Sliding motion related to bit-sticking phenomena

The bit-sticking phenomenon is represented by setting $\dot{x}_5 = x_5 = 0$ in the last equation of (9). Under this condition, due to Eq. (7), a sliding motion may appear. This regime can be stated by means of the discontinuity or switching surface, $\Sigma$, and the sliding region $\tilde{\Sigma} \subset \Sigma$, with:

$$\sigma(\mathbf{x}) = x_5, \ \Sigma := \{\mathbf{x} \in \mathbb{R}^5 : \sigma(\mathbf{x}) = 0\},$$
$$\tilde{\Sigma} = \{\mathbf{x} \in \Sigma : |k_{tb}x_4 + c_{tb}x_3| < W_{ob}R_b\mu_{s_b}\}. \tag{12}$$

$\tilde{\Sigma}$ is the set where a sliding motion can take place. The complement of $\tilde{\Sigma}$ in $\Sigma$ is usually referred to as *crossing set* [25] and is the set of all $\mathbf{x} \in \Sigma$ at which the trajectory of the system crosses $\Sigma$ without sliding. The boundaries of $\tilde{\Sigma}$ are denoted by $\partial\tilde{\Sigma}^+$ and $\partial\tilde{\Sigma}^-$, with:

$$\partial\tilde{\Sigma}^+ = \{\mathbf{x} \in \tilde{\Sigma} : k_{tb}x_4 + c_{tb}x_3 = W_{ob}R_b\mu_{s_b}\},$$
$$\partial\tilde{\Sigma}^- = \{\mathbf{x} \in \tilde{\Sigma} : k_{tb}x_4 + c_{tb}x_3 = -W_{ob}R_b\mu_{s_b}\}.$$

The system dynamics on $\Sigma$ have the form $\dot{\mathbf{x}} = \mathbf{f}_s(\mathbf{x}, u)$, where $\mathbf{f}_s$ is the equivalent dynamics on $\Sigma$ [26,27]. For velocities $x_5 \neq 0$, the dynamics of system (9) are described by:

$$\dot{\mathbf{x}} = \begin{cases} \mathbf{f}^+(\mathbf{x}, \mu) & \text{if } \mathbf{x} \in \mathcal{X}^+, \\ \mathbf{f}^-(\mathbf{x}, \mu) & \text{if } \mathbf{x} \in \mathcal{X}^-, \end{cases} \tag{13}$$

with $\mu = W_{ob} \times u \in \mathbb{R}^2$ the parameter vector and,

$$\mathbf{f}^+(\mathbf{x}, \mu) = \mathbf{A}\mathbf{x} + \mathbf{B}u + \mathbf{T}_f(\mathbf{x})|_{T_{f_b}=T_{f_b}^+},$$
$$\mathbf{f}^-(\mathbf{x}, \mu) = \mathbf{A}\mathbf{x} + \mathbf{B}u + \mathbf{T}_f(\mathbf{x})|_{T_{f_b}=T_{f_b}^-}, \tag{14}$$
$$\mathcal{X}^+ = \{\mathbf{x} \in \mathbb{R}^5 : x_5 > 0\}, \quad \mathcal{X}^- = \{\mathbf{x} \in \mathbb{R}^5 : x_5 < 0\}.$$

Functions $\mathbf{f}^+, \mathbf{f}^-$ are continuous and smooth and $\mathbf{f}^+ \neq \mathbf{f}^-$ on $\Sigma$.

### 3.1.1. Properties of the sliding regime

**Proposition 1.** *System (9) with (7) is considered and the following set is defined:*

$$\mathcal{S} := \left\{ \mathbf{x} \in \mathbb{R}^5 : |c_{t_b}x_3 + k_{tb}x_4| < (c_{tb} + c_b)|x_5| + W_{ob}R_b\mu_b(x_5) \right\}, \tag{15}$$

*with $\mu_b(x_5)$ as defined in (4). If $\mathbf{x} \in \mathcal{S}$ then the system trajectory enters a sliding motion on $\tilde{\Sigma} \subset \Sigma$.*

**Proof.** $\dot{\sigma}$ denotes the derivative of $\sigma$ along the trajectories of the system. First, it will be shown that $\forall\mathbf{x} \in \mathcal{S}, \sigma(\mathbf{x})\dot{\sigma}(\mathbf{x}) < 0$, that is, that a sliding mode can exist. From (9), it is obtained:

$$\dot{\sigma} = \frac{1}{J_b}\left[ c_{tb}x_3 + k_{tb}x_4 - (c_{tb} + c_b)x_5 - T_{f_b}(x_5) \right]. \tag{16}$$

Two cases are considered:

- Case 1: $\sigma < 0$. Then $x_5 < 0$ and $T_{f_b} = T_{f_b}^-$. Consequently, $\dot{\sigma} > 0$ in the set,

$$\left\{ \mathbf{x} \in \mathbb{R}^5 : \ |c_{t_b} x_3 + k_{tb} x_4| < (c_{tb} + c_b)|x_5| + \left[ T_{c_b} + (T_{s_b} - T_{c_b}) \exp^{\frac{\gamma_b}{v_f} x_5} \right] \right\}. \tag{17}$$

- Case 2: $\sigma > 0$. Then $x_5 > 0$ and $T_{f_b} = T_{f_b}^+$. Hence, $\dot{\sigma} < 0$ in the set,

$$\left\{ \mathbf{x} \in \mathbb{R}^5 : \ |c_{t_b} x_3 + k_{tb} x_4| < (c_{tb} + c_b)|x_5| + \left[ T_{c_b} + (T_{s_b} - T_{c_b}) \exp^{-\frac{\gamma_b}{v_f} x_5} \right] \right\}. \tag{18}$$

Combining both cases, $\sigma\dot{\sigma} < 0$ in the set $\mathscr{S}$ as defined in (15).

$T_{fb_{eq}}$ stands for the solution for $T_{f_b}$ of equation $\dot{\sigma} = 0$. Since $\sigma\dot{\sigma} < 0$ and $T_{f_b}^- < T_{fb_{eq}} < T_{f_b}^+$ in the set $\mathscr{S}$, a sliding motion takes place when the system trajectory hits the surface $\sigma = 0$ at $\mathbf{x} \in \mathscr{S}$. The sliding region is $\tilde{\Sigma} \subset \mathscr{S}$.

In addition, any trajectory eventually hits the surface $\sigma = 0$ at an $\mathbf{x}$ within the set $\mathscr{S}$. Consider that $\mathbf{x} \in \mathscr{S}$. Suppose that, at a certain time, $\sigma < 0$, then the system is described by $\dot{\mathbf{x}} = \mathbf{f}^-(\mathbf{x}, W_{ob}, u)$ and $\dot{\sigma} > 0$. Hence, $\sigma$ increases until it eventually gets zero, hitting the surface $\sigma = 0$. On the other hand, if $\sigma > 0$, the system is described by $\dot{\mathbf{x}} = \mathbf{f}^+(\mathbf{x}, W_{ob}, u)$ and $\dot{\sigma} < 0$. Consequently, at some time, $\sigma$ starts decreasing until it eventually crosses zero and hits $\sigma = 0$. Therefore, any trajectory of the system within the set $\mathscr{S}$ enters a sliding regime on $\tilde{\Sigma}$. Hereinafter, the set $\mathscr{S}$ will be referred to as the region of attraction of $\tilde{\Sigma}$. □

**Remark 2.** Proposition 1 does not assert that if the system trajectory goes into the sliding regime on the surface $\Sigma$ then it remains there. The trajectory may leave the sliding mode. However, if this happens, the trajectory may eventually return to the surface. In addition, the trajectory intersects the surface $\sigma = 0$ entering in a sliding regime from the set $\mathcal{X}_{34}^+$, with $\mathcal{X}_{34}^+ = \{ \mathbf{x} \in \mathcal{X}^+ : \ x_3 > 0, x_4 > 0 \}$. This can be shown by contradiction. Suppose that $x_3 > 0$ and $x_4 > 0$ and the trajectory hits the surface $\sigma = 0$ and no sliding motion is established, that is, the trajectory crosses the surface. Hence, at the crossing point, it must be met that when passing from $\sigma > 0$ to $\sigma < 0$, $\dot{\sigma} < 0$ must be maintained. When $\sigma < 0$, $\dot{\sigma}$ has the form,

$$\dot{\sigma} = \frac{1}{J_b} \left[ c_{tb} x_3 + k_{tb} x_4 - (c_{tb} + c_b)x_5 - T_{f_b}^-(x_5) \right]. \tag{19}$$

From (19), $\dot{\sigma}$ is negative if either $x_3 < 0$ or $x_4 < 0$ (or both). This fact contradicts the supposition. Consequently, after a certain time, the trajectory may enter a sliding regime from the set $\mathcal{X}_{34}^+$.

**Remark 3.** Once the trajectory of the system is in a sliding regime, the sliding surface $\tilde{\Sigma}$ can change from being attractive (stable) to be repulsive (unstable), and due to this fact the system trajectory can leave the sliding motion [25,27]. $\tilde{\Sigma}$ is attractive $\forall \mathbf{x} \in \mathscr{S}$. From the form of $\mathscr{S}$ in (15), it can be appreciated that $W_{ob}$ is a key parameter determining the attractivity of $\tilde{\Sigma}$. The higher the $W_{ob}$ is, the more likely is $\tilde{\Sigma}$ to be attractive, which is a nondesired situation in the drillstring.

### 3.1.2. System equilibria within and outside the switching surface

Two types of equilibria are identified. On the one hand, the equilibria on the switching surface $\Sigma$. On the other hand, the standard equilibrium, outside $\Sigma$, when the velocities are positive.

Three main kinds of equilibria are identified on $\Sigma$: (1) a unique quasiequilibrium point for each $u$, (3) boundary equilibria, (2) tangent points.

**Definition 4** ([25,27]). System (13) with (14) is considered. $\overline{\mathbf{x}} \in \mathbb{R}^5$ is referred to as the standard equilibrium point of the system if there exists $(\overline{W}_{ob}, \overline{u}) \in \mathbb{R}^2$ such that $\mathbf{f}^+(\overline{\mathbf{x}}, \overline{W}_{ob}, \overline{u}) = 0$ or $\mathbf{f}^-(\overline{\mathbf{x}}, \overline{W}_{ob}, \overline{u}) = 0$. Let $\tilde{\mathbf{x}} \in \mathbb{R}^5$, $\tilde{u} \in \mathbb{R}$ be such that $\mathbf{f_s}(\tilde{\mathbf{x}}, \tilde{u}) = 0$ and $\sigma(\tilde{\mathbf{x}}) = 0$. $\tilde{\mathbf{x}}$ is said to be a real quasiequilibrium point if $\tilde{\mathbf{x}} \in \tilde{\Sigma}$. If $\tilde{\mathbf{x}} \notin \tilde{\Sigma}$, $\tilde{\mathbf{x}}$ is referred to as virtual quasiequilibrium point. $\mathbf{x}_B \in \Sigma$ for which one of the vectors $\mathbf{f}^+$, $\mathbf{f}^-$ vanishes is referred to as boundary equilibrium. $\mathbf{x}_T \in \Sigma$ for which the vectors $\mathbf{f}^+$, $\mathbf{f}^-$ are nonzero but one of them is tangent to $\Sigma$ is referred to as tangent point.

The quasiequilibrium point $\tilde{\mathbf{x}} \in \Sigma$ has the form:

$$\tilde{x}_1 = \tilde{x}_3 = \tilde{x}_5 = 0, \quad \tilde{x}_2 = \frac{u}{k_t}, \quad \tilde{x}_4 = \frac{u}{k_{tb}}. \tag{20}$$

**Proposition 5.** The quasiequilibrium point $\tilde{\mathbf{x}} \in \Sigma$ given by (20) is asymptotically stable.

**Proof.** The following Lyapunov function is considered, which corresponds to the sum of the kinetic and potential energy of the system on $\Sigma$:

$$V(\mathbf{x}, \tilde{\mathbf{x}}) = \frac{1}{2} \left\{ k_t(x_2 - \tilde{x}_2)^2 + k_{tb}(x_4 - \tilde{x}_4)^2 + J_r x_1^2 + J_p x_3^2 \right\}. \tag{21}$$

The derivative of $V$ along the trajectories of $\dot{\mathbf{x}} = \mathbf{f_s}(\mathbf{x}, u)$ is:

$$\dot{V}(\mathbf{x}) = -c_r x_1^2 - c_{tb} x_3^2 - c_t(x_1 - x_3)^2. \tag{22}$$

Consequently, $\dot{V}(\mathbf{x}) \leq 0$. Due to the fact that $\dot{V}(\mathbf{x}) = 0$ only for $\mathbf{x} = \tilde{\mathbf{x}}$, by LaSalle's invariance principle [28], the quasiequilibrium $\tilde{\mathbf{x}}$ is asymptotically stable.

Furthermore, let define the following set: $\mathcal{A} := \{\mathbf{x} \in \mathbb{R}^5 : V(\mathbf{x}, \tilde{\mathbf{x}}) < r\}$, where $r$ is the maximum value for which $\mathcal{A} \subset \Sigma$. It can be said that if the system trajectory intersects the surface $\Sigma$ at some time inside the set $\mathcal{A}$, the trajectory remains in the surface and from that time it tends asymptotically towards $\tilde{\mathbf{x}}$ [28].   □

**Remark 6.** If the trajectory intersects the sliding surface $\tilde{\Sigma}$ at a point which does not belong to $\mathcal{A}$, the trajectory eventually converges towards $\tilde{\mathbf{x}}$. However, it may go out of the surface several times before reaching the set $\mathcal{A}$. If $\tilde{\mathbf{x}}$ is virtual and far away enough from the boundary of $\tilde{\Sigma}$, the trajectory is likely to leave the sliding motion. If the trajectory goes out of the sliding regime, it may eventually come back to the sliding surface depending on: (1) the attractivity of $\tilde{\Sigma}$, and (2) the stability characteristics of the standard equilibrium (see Section 3.2).

The set of boundary equilibria $\mathbf{x}_B$ is the set of quasiequilibria $\tilde{\mathbf{x}}$ for which $|u| = T_{s_b}$. By considering $\dot{\mathbf{x}} = 0$ in (9), the following set of equilibria is obtained:

$$\mathcal{X}_0 = \left\{ \mathbf{x} \in \mathbb{R}^5 : x_2 \in \left[ -\frac{T_{s_b}}{k_t}, \frac{T_{s_b}}{k_t} \right], \; x_4 \in \left[ -\frac{T_{s_b}}{k_{tb}}, \frac{T_{s_b}}{k_{tb}} \right], \; x_1 = x_3 = x_5 = 0 \right\}$$

$$|u| \leq T_{s_b}.$$

Notice that $\mathcal{X}_0 / \partial \mathcal{X}_0 \subset \tilde{\Sigma}$ and the boundary equilibria $\mathbf{x}_B \in \partial \mathcal{X}_0$. Finally, the tangent points, $\mathbf{x}_T$, belong to the boundary of $\tilde{\Sigma}$.

A quasiequilibrium $\tilde{\mathbf{x}}$ collides with a boundary equilibrium when $\tilde{\mathbf{x}}$ is at the boundary of $\tilde{\Sigma}$. No other local bifurcation (in the sense of [25]) of these points occurs on $\Sigma$.

The fact that the quasiequilibrium $\tilde{\mathbf{x}}$ is asymptotically stable implies that if $\tilde{\mathbf{x}} \in \tilde{\Sigma}$, the bit will be permanently stuck. On the other hand, the bit will move with a constant positive velocity (convergence to the standard equilibrium) when $\tilde{\mathbf{x}} \notin \tilde{\Sigma}$ and is far away from the boundary of $\tilde{\Sigma}$. Such a condition is accomplished when $u$ is sufficiently larger than $T_{s_b}$ [10].

The standard equilibrium for $x_5 > 0$, $\bar{\mathbf{x}} \in \mathbb{R}^5$, such that $\mathbf{f}^+(\bar{\mathbf{x}}, W_{ob}, u) = 0$ is:

$$\bar{x}_1 = \bar{x}_3 = \bar{x}_5 > 0, \qquad u - T_{f_b}^+(x_5, W_{ob})\Big|_{x_5 = \bar{x}_5} - (c_r + c_b)\bar{x}_5 = 0,$$

$$\bar{x}_2 = \frac{h(\bar{x}_5, W_{ob}, u)}{k_t}, \qquad \bar{x}_4 = \frac{h(\bar{x}_5, W_{ob}, u)}{k_{tb}}, \tag{23}$$

with $h(\bar{x}_5, W_{ob}, u) = \left[ c_r T_{f_b}^+(x_5, W_{ob})\Big|_{x_5 = \bar{x}_5} + c_b u \right] / (c_r + c_b)$ and $u > T_{s_b} > 0$.

The equilibrium $\bar{x}$ is locally asymptotically stable depending on $W_{ob}$, $u$ and $\bar{x}_5$. This will be studied in Section 3.2. Furthermore, the distance between $\bar{\mathbf{x}}$ and the boundary of $\mathcal{S}$ influences in the number of times the trajectory enters $\tilde{\Sigma}$ before converging to $\bar{\mathbf{x}}$.

### 3.1.3. Sliding-mode-related dynamical regimes

The characteristics of $\tilde{\Sigma}$, $\tilde{\mathbf{x}}$, $\mathcal{S}$ and $\bar{\mathbf{x}}$ and the relationships among them define three dynamical regimes:

- *Stick-slip* at $x_5$, that is, the trajectory enters and leaves repeatedly the sliding mode. In this case, $\bar{x}$ can be unstable or stable with a small domain of attraction, $\tilde{\Sigma}$ alternates among being repulsive or attractive, $\tilde{\mathbf{x}}$ is next to $\partial \tilde{\Sigma}^+$. From simulations by using parameters (11), it is obtained that $\bar{\mathbf{x}}$ belongs to the boundary of $\mathcal{S}$ and that the sliding periodic orbit encircles $\bar{\mathbf{x}}$. Hence, if the system trajectory is in the sliding motion ($\tilde{\Sigma}$ is attractive), when the trajectory approaches $\tilde{\mathbf{x}}$, it can leave the sliding domain, and then, $\tilde{\Sigma}$ becomes repulsive (see Fig. 4) and the trajectory eventually moves towards $\bar{\mathbf{x}}$. If the domain of attraction of $\bar{\mathbf{x}}$ is not big enough or the equilibrium is unstable, the trajectory may not reach it. Moreover, when the bit velocity increases and gets its maximum value, $\tilde{\Sigma}$ becomes attractive, and the trajectory falls again into the sliding domain. This is repeated continuously.
- *Permanent stuck bit*, i.e., $\mathbf{x}(t) \in \tilde{\Sigma}$ after certain time. In this case, $\bar{\mathbf{x}}$ can be unstable or stable with a small domain of attraction, after certain time $\tilde{\Sigma}$ is attractive, $\tilde{\mathbf{x}} \in \tilde{\Sigma}$ and $\tilde{\mathbf{x}}$ is far away enough from $\partial \tilde{\Sigma}^+$. If the system is in the sliding motion then the system trajectories tend asymptotically to $\tilde{\mathbf{x}}$. Depending on the distance between $\tilde{\mathbf{x}}$ and $\partial \Sigma^+$, the trajectories may enter and leave $\tilde{\Sigma}$ several times before remaining on it, each time the trajectory enters $\tilde{\Sigma}$, it will be closer to $\mathcal{A}$, which is the domain of attraction of $\tilde{\mathbf{x}}$.
- After certain time, $\mathbf{x}(t)$ *converges to* $\bar{\mathbf{x}}$. In this case, $\bar{\mathbf{x}}$ is locally asymptotically stable, $\tilde{\Sigma}$ becomes repulsive after certain time, $\tilde{\mathbf{x}} \notin \tilde{\Sigma}$ and $\tilde{\mathbf{x}}$ is far away enough from $\partial \tilde{\Sigma}^+$ ($u$ is sufficiently larger than $T_{s_b}$). If the system is in the sliding motion and the trajectories move towards $\tilde{\mathbf{x}}$, they can leave the sliding domain and fall into the domain of attraction of $\bar{\mathbf{x}}$. Depending on the distance between $\tilde{\mathbf{x}}$ and $\partial \Sigma^+$, and on the distance between $\bar{\mathbf{x}}$ and the boundary of $\mathcal{S}$, the trajectories may enter and leave $\tilde{\Sigma}$ several times before converging to $\bar{\mathbf{x}}$.
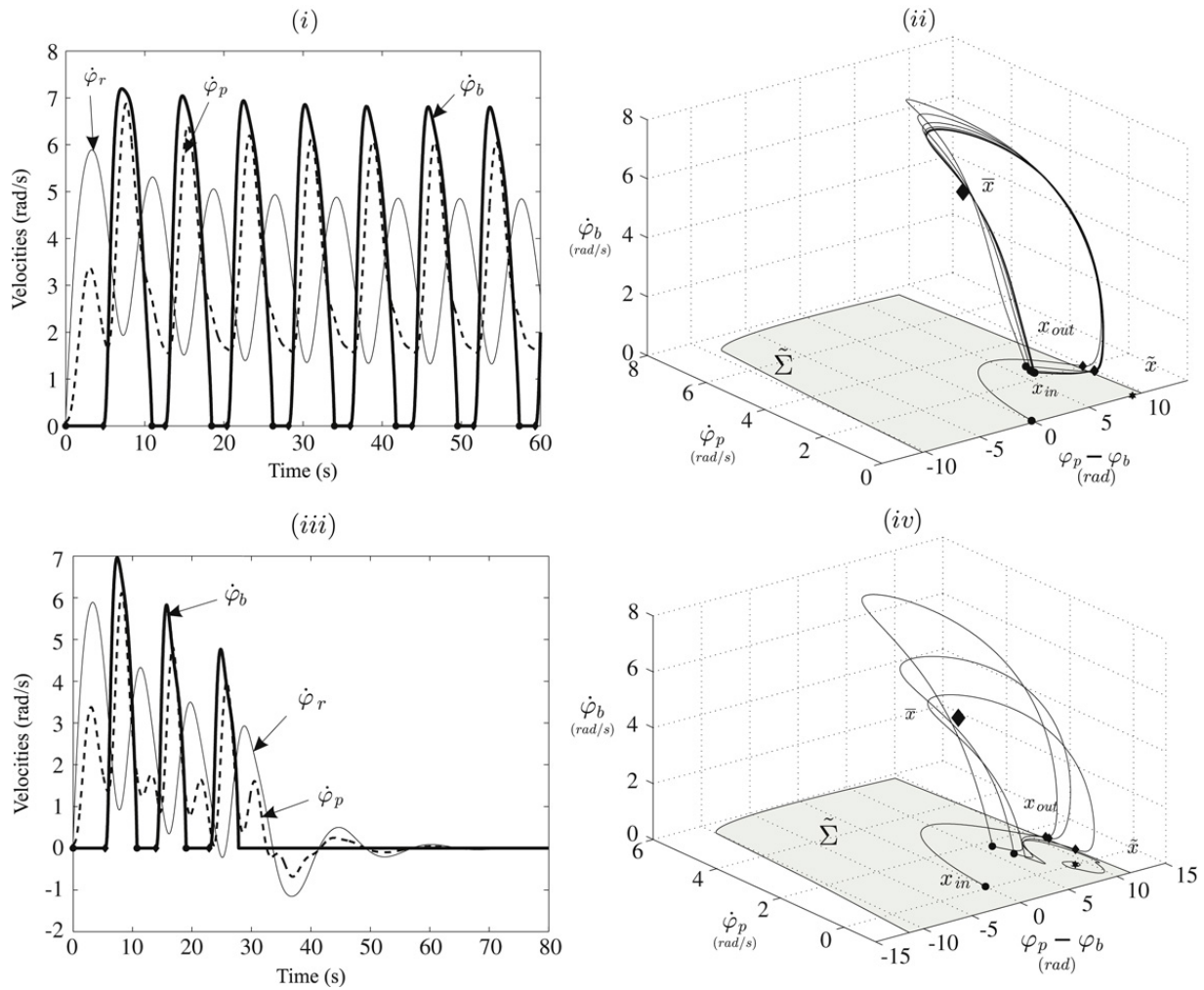
**Fig. 2.** Bit-sticking phenomena in system (9): (i), (ii) stick-slip situation; (iii), (iv) permanent stuck bit. $\mathbf{x}_{in}$ (●) and $\mathbf{x}_{out}$ (♦) are the points at which the system trajectory enters and goes out of the sliding region. ♦ standard equilibrium ($\bar{\mathbf{x}}$). ★ quasiequilibrium point ($\tilde{\mathbf{x}}$), $\tilde{\Sigma}$ (shadowed region).
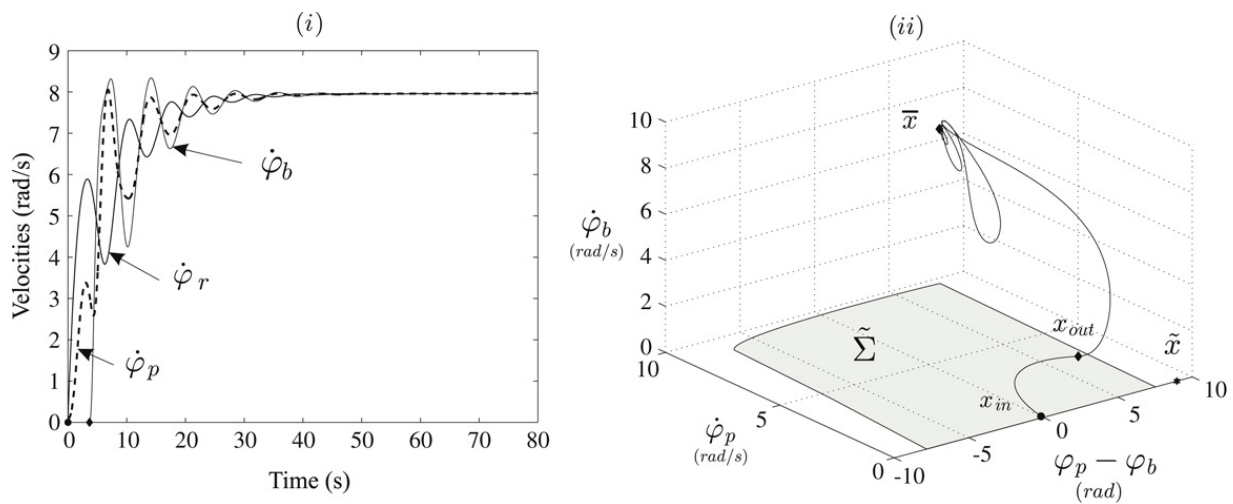


**Fig. 3.** Convergence to the standard equilibrium point $\bar{x}$ for positive velocities. ●$\mathbf{x}_{in}$, ♦$\mathbf{x}_{out}$, ♦ standard equilibrium ($\bar{\mathbf{x}}$), ★ quasiequilibrium point ($\tilde{\mathbf{x}}$), $\tilde{\Sigma}$ (shadowed region).

The two sticking bit situations are shown in Fig. 2. In Fig. 3, the situation of the convergence of the trajectory to $\bar{\mathbf{x}}$ is depicted. Parameters (11) are used, as well as, $u = 8138$ Nm, $W_{ob} = 74\,386$ N for the stick-slip case, $W_{ob} = 82\,000$ N for the stuck-bit case, and $W_{ob} = 70\,389$ N for the convergence to $\bar{\mathbf{x}}$. In the simulations, $\bar{\mathbf{x}}$ is obtained by using the Newton–Raphson method.
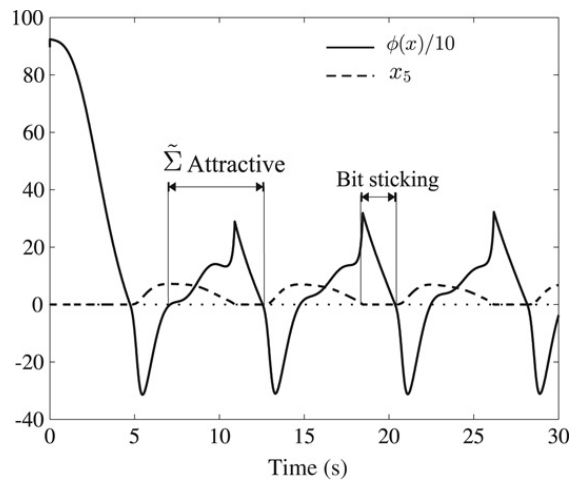
**Fig. 4.** Change of the attractivity of $\tilde{\Sigma}$ when the bit is in stick-slip motion. When $\phi(\mathbf{x}) > 0$, $\tilde{\Sigma}$ is attractive. Otherwise, $\tilde{\Sigma}$ is repulsive. $\phi(\mathbf{x}) = (c_{\text{tb}} + c_b)|x_5| + W_{\text{ob}} R_b \mu_b(x_5) - |c_{\text{tb}} x_3 + k_{\text{tb}} x_4|$.
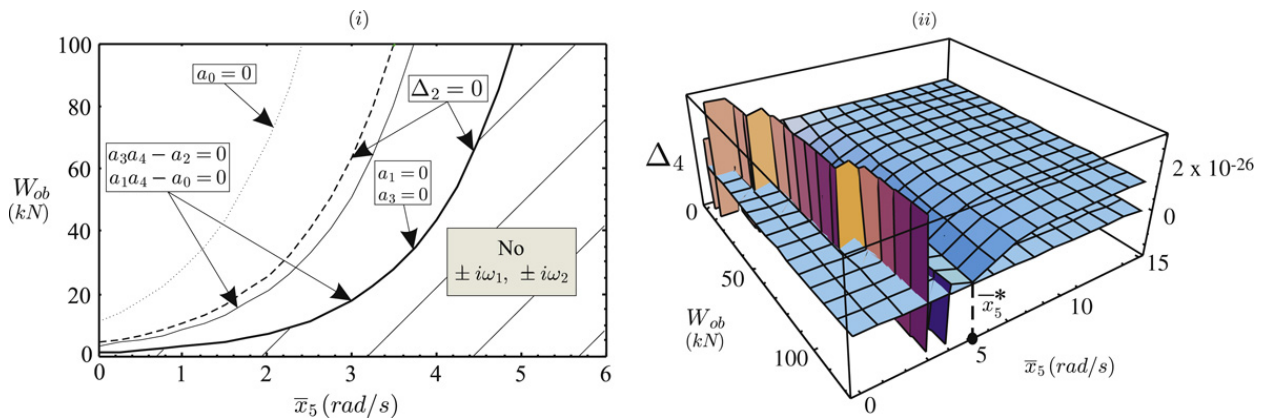


**Fig. 5.** Local stability of $\bar{\mathbf{x}}$: (i) $(\bar{x}_5, W_{\text{ob}})$ for which there are no two pairs of complex conjugate eigenvalues crossing the imaginary axis; these $(\bar{x}_5, W_{\text{ob}})$ are also those for which some of the conditions (25) are satisfied (wide-lined region), (ii) evaluation of $\Delta_4$ for parameters (11) for varying $(\bar{x}_5, W_{\text{ob}})$.

### 3.2. Stability analysis for velocities greater than zero

The standard equilibrium $\bar{\mathbf{x}}$ is locally asymptotically stable depending on $W_{\text{ob}}$, $u$ and $\bar{x}_5$. The loss of stability of $\bar{\mathbf{x}}$ is mainly due to the presence of Hopf bifurcations (HB). In particular, multiple subcritical HB's give rise to branches of unstable periodic orbits.

The characteristic polynomial of the Jacobian matrix of system (10) at the standard equilibrium $\bar{\mathbf{x}}$ (23) is considered as:

$$\lambda^5 + a_4\lambda^4 + a_3\lambda^3 + a_2\lambda^2 + a_1\lambda + a_0 = 0, \tag{24}$$

with $a_i$, $i = 0, \ldots, 4$, depending on system physical parameters, $\bar{x}_5$ and $W_{\text{ob}}$. The local asymptotic stability of $\bar{\mathbf{x}}$ can be ensured by means of the Liénard–Chipart criterion [29], that is, when:

$$a_0 > 0, \, a_1 > 0, \, a_3 > 0, \, \Delta_2 = a_1a_2 - a_0a_3 > 0,$$
$$\Delta_4 = \Delta_2(a_3a_4 - a_2) - (a_0 - a_1a_4)^2 > 0. \tag{25}$$

From (25), safe ranges of the $W_{\text{ob}}$ and velocities at the equilibrium ($\bar{x}_5$) can be identified (see Fig. 5.(i) and 5.(ii)). For the 3-DOF system, the Hurwitz determinant $\Delta_4$ is numerically evaluated for varying $(\bar{x}_5, W_{\text{ob}})$. It is concluded that for enough high values of $\bar{x}_5$ ($\bar{x}_5 > \bar{x}_5^*$) and low enough values of $W_{\text{ob}}$, $\bar{\mathbf{x}}$ is locally asymptotically stable.

Different types of HB's can be detected. We focus on simple and double HB's [30]. A simple HB is presented when a pair of complex conjugate eigenvalues of the Jacobian matrix crosses the imaginary axis while all other eigenvalues have negative real parts. Otherwise, a double HB arises when two pairs of complex conjugate eigenvalues cross the imaginary axis.

The presence of a simple HB is determined by the condition $\Delta_4 = 0$ [30], i.e., when $a_3a_4 - a_2 = 0$ and $a_0 - a_1a_4 = 0$, or when $\Delta_2 = 0$ and $a_0 - a_1a_4 = 0$. Although they are not the only conditions to accomplish, these conditions could guide us to establish an estimation of the $W_{\text{ob}}$ and the rotary velocities for which $\bar{\mathbf{x}}$ might not undergo a simple HB. Furthermore, a double HB may appear when the solutions of (24) are of the form $\lambda = \pm i\omega_j$, $\lambda = \alpha \in \mathbb{R}$, with $j = 1, 2$. This is accomplished
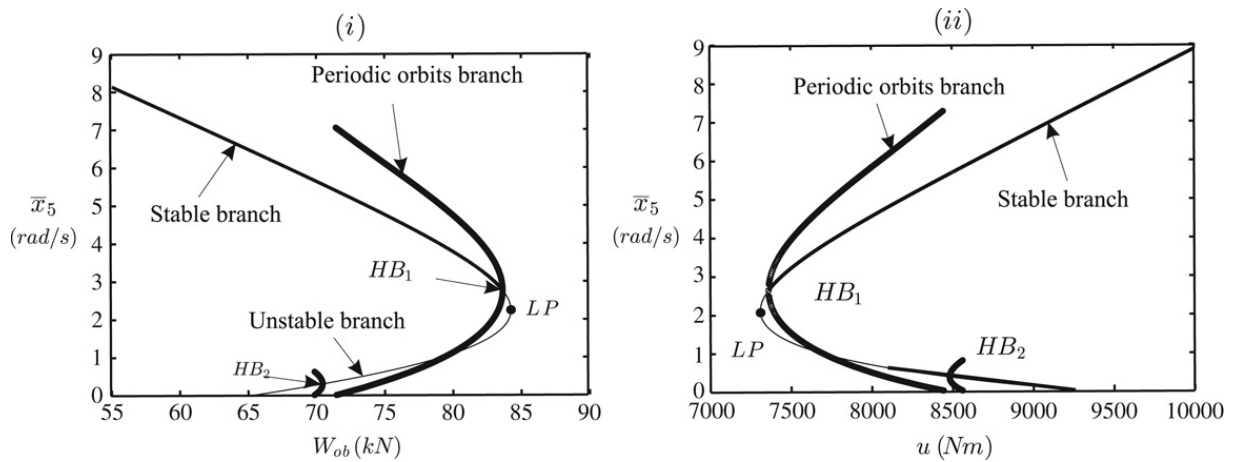
**Fig. 6.** Bifurcation diagrams: (i) $(W_{ob}, \bar{x}_5)$ for a fixed $u = 8138$ N m, (ii) $(u, \bar{x}_5)$ for a fixed $W_{ob} = 74\,386$ N.
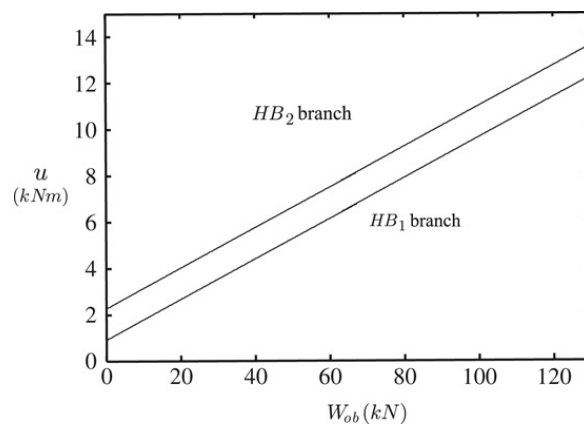


**Fig. 7.** Values $(W_{ob}, u)$ at which a HB can appear.

when $a_3 a_4 - a_2 = 0$ and $a_0 - a_1 a_4 = 0$. In conclusion, the stability region of $\bar{\mathbf{x}}$ corresponds to low values of $W_{ob}$ and high enough values of the rotary velocities. This can be appreciated in Fig. 5.(i) and 5.(ii).

The torque $u$ is the third parameter which can be analysed in order to establish the stability of $\bar{\mathbf{x}}$. The bifurcation diagram of $(W_{ob}, \bar{x}_5)$ for a fixed $u$ is shown in Fig. 6.(i). For each value of $u$, a different bifurcation diagram is obtained. The bifurcation diagram of $(u, \bar{x}_5)$ and a fixed $W_{ob}$ is depicted in Fig. 6.(ii). The stable branches represent the values of $(W_{ob}, \bar{x}_5)$ and $(u, \bar{x}_5)$ for which $\bar{\mathbf{x}}$ is stable. The unstable branches represent the values of the parameters for which $\bar{\mathbf{x}}$ is unstable. To conclude with, the equilibrium $\bar{\mathbf{x}}$ is stable when: (1) for a fixed $u$, the $W_{ob}$ is small enough, (2) for a fixed $W_{ob}$, the torque $u$ is large enough. For such ranges of parameters, bit-sticking problems are avoided.

The values $(W_{ob}, u)$ for which a HB point appear can be also obtained. In Fig. 7, two branches of HB points are depicted, one for $HB_1$ and another for $HB_2$ (Fig. 6). These branches are the origin of oscillations in the system. For each pair of $(W_{ob}, u)$ a different set of periodic orbits can be obtained. The bifurcation diagrams have been obtained with XPPAUT [31].

## 4. Linear PI-type control to eliminate nondesired transitions

The control goals are to eliminate bit-sticking phenomena and to drive the bit velocity to a desired value. This is accomplished by means of the following control with an adequate selection of controller parameters:

$$u = K_1 x_6 + K_2(\Omega - x_1) + K_3(x_1 - x_5) + u^*,$$
$$x_6 = \int_0^t [\Omega - x_1(\tau)]\,d\tau, \ \dot{x}_6 = \Omega - x_1, \tag{26}$$

with $\Omega > 0$ the desired velocity value, $K_i$, $i = 1, 2, 3$, positive constants and $u^* > 0$ is a constant value obtained from the sliding motion characteristics in the open-loop system. $u^* = W_{ob} R_b \mu_{s_b} = T_{s_b}$ is the minimum value of $u$ for the system trajectory to cross the boundary $\partial\tilde{\Sigma}^+$ and leave $\tilde{\Sigma}$. This value of $u^*$ prevents the bit from sticking when control (26) is initially switched on.

The closed-loop system state vector $\mathbf{x}_c$ is defined as,

$$\mathbf{x}_c = (\dot{\varphi}_r, \varphi_r - \varphi_p, \dot{\varphi}_p, \varphi_p - \varphi_b, \dot{\varphi}_b, x_6)^T = (x_{c,1}, x_{c,2}, x_{c,3}, x_{c,4}, x_{c,5}, x_{c,6})^T. \tag{27}$$

By substituting (26) in (9), the closed-loop system is obtained as,

$$\dot{\mathbf{x}}_c(t) = \mathbf{A}_c \mathbf{x}_c(t) + \mathbf{T}_{fc}(\mathbf{x}_c(t)). \tag{28}$$

The dynamical changes introduced by control (26) in the open-loop system are, mainly: (1) the closed-loop standard equilibrium point ($\bar{\mathbf{x}}_c$) has the angular velocities equal to $\Omega$; (2) there is no quasiequilibrium point on the switching surface $\Sigma$ ($\tilde{\mathbf{x}}$ disappears), consequently, the permanent stuck-bit situation is eliminated; (3) periodic orbits may still arise in the system, due to the loss of stability of $\bar{\mathbf{x}}_c$, basically depending on the values of $K_2$, $K_3$, $W_{ob}$ and $\Omega$; (4) $\bar{\mathbf{x}}_c$ belongs to the boundary of $\mathcal{S}$.

As was established in Section 3, ensuring the local stability of the standard equilibrium point is essential in order not to have stick-slip oscillations. Moreover, the properties of the existing sliding regime are key issues to fully understand the closed-loop system response.

### 4.1. Sliding motion and equilibrium characteristics

In the closed-loop system, the sliding region $\tilde{\Sigma}$ is maintained and the parameter $W_{ob}$ will play a key role on the attractivity of $\tilde{\Sigma}$. The dynamics of system (28) while evolving on $\Sigma$ are obtained by means of the Utkin's equivalent control method [26, 27] and has the form,

$$\mathbf{f}_{sc}(\mathbf{x}_c, K_1, K_2, K_3) = \mathbf{A}_c \mathbf{x}_c + \mathbf{T}_{fc}(\mathbf{x}_c)|_{T_{f_b} = T_{fbeq}}, \tag{29}$$

where

$$T_{fbeq}(\mathbf{x}_c) = c_{tb} x_{c,3} + k_{tb} x_{c,4} - (c_{tb} + c_b) x_{c,5}. \tag{30}$$

Now, there is no quasiequilibrium $\tilde{\mathbf{x}}_c$ such that $\mathbf{f}_{sc}(\tilde{\mathbf{x}}_c, K_1, K_2, K_3) = 0$. Therefore, the permanent stuck-bit situation is avoided.

Stick-slip oscillations may appear in the closed-loop system due to the existence of the sliding region $\tilde{\Sigma}$ which can become locally attractive, in addition to the existence of a standard equilibrium which can become unstable or whose domain of attraction can be reduced due to the variation of some parameters. The closed-loop system has a unique standard equilibrium point for $x_5 > 0, \bar{\mathbf{x}}_c \in \mathbb{R}^6$, with:

$$
\begin{aligned}
&\bar{x}_{c,1} = \bar{x}_{c,3} = \bar{x}_{c,5} = \Omega, \\
&\bar{x}_{c,2} = \frac{h(\Omega, W_{ob})}{k_t}, \bar{x}_{c,4} = \frac{h(\Omega, W_{ob})}{k_{tb}}, \ h(\Omega, W_{ob}) = \left[ c_b \Omega + T_{f_b}^+(x_5, W_{ob})\Big|_{x_5 = \Omega} \right], \\
&\bar{x}_{c,6} = \frac{1}{K_1} \left[ (c_r + c_b)\Omega + T_{f_b}^+(x_5, W_{ob})\Big|_{x_5 = \Omega} - u^* \right],
\end{aligned} \tag{31}
$$

with $T_{f_b}^+$ as defined in (8).

Two dynamical regimes are highlighted:

- *Stick-slip periodic motion.* If the system trajectory is in the sliding region, it can approach its boundary and leave the sliding domain, due to the loss of attractivity of $\tilde{\Sigma}$. Then, it eventually tends to the standard equilibrium point $\bar{\mathbf{x}}_c$. If the domain of attraction of $\bar{\mathbf{x}}_c$ is not big enough or the equilibrium is unstable, the trajectory may not reach it and fall again into the sliding domain due to the fact that $\tilde{\Sigma}$ becomes attractive with increasing velocities (Fig. 8). This is repeated continuously, and it gives rise to the stick-slip motion (Fig. 8).
- *The angular velocities are equal to $\Omega$.* $\bar{\mathbf{x}}_c$ is locally asymptotically stable. If the system trajectory is in the sliding region, it can eventually leave the sliding region $\tilde{\Sigma}$, which becomes repulsive due to the increase of $x_{c,3}$ and $x_{c,4}$ along $\Sigma$, and can fall into the domain of attraction of the equilibrium $\bar{\mathbf{x}}_c$ provided that this domain is big enough. Depending on the relationships between the domain of attraction of $\bar{\mathbf{x}}_c$ and the set $\mathcal{S}$, the trajectory may enter and leave $\tilde{\Sigma}$ several times before converging to $\bar{\mathbf{x}}_c$. In Fig. 9, the influence of the value $u^*$ in the control is appreciated. If $u^*$ were not considered, an initial stuck-bit region would appear. When the rotary velocities reach the value $\Omega$, the control $u$ is greater than $u^*$.

The changes in the stability properties of $\bar{\mathbf{x}}_c$ are determined by the changes in the parameters $K_2$, $K_3$, $\Omega$ and $W_{ob}$. This will be analysed in the next section.

### 4.2. Stability analysis and controller parameter selection

The stability properties of $\bar{\mathbf{x}}_c$ can be studied locally by means of the linearized controlled system around it. The characteristic polynomial of the Jacobian matrix of system (28) at $\bar{\mathbf{x}}_c$ has the following form:

$$\lambda^6 + b_5 \lambda^5 + b_4 \lambda^4 + b_3 \lambda^3 + b_2 \lambda^2 + b_1 \lambda + b_0 = 0, \tag{32}$$
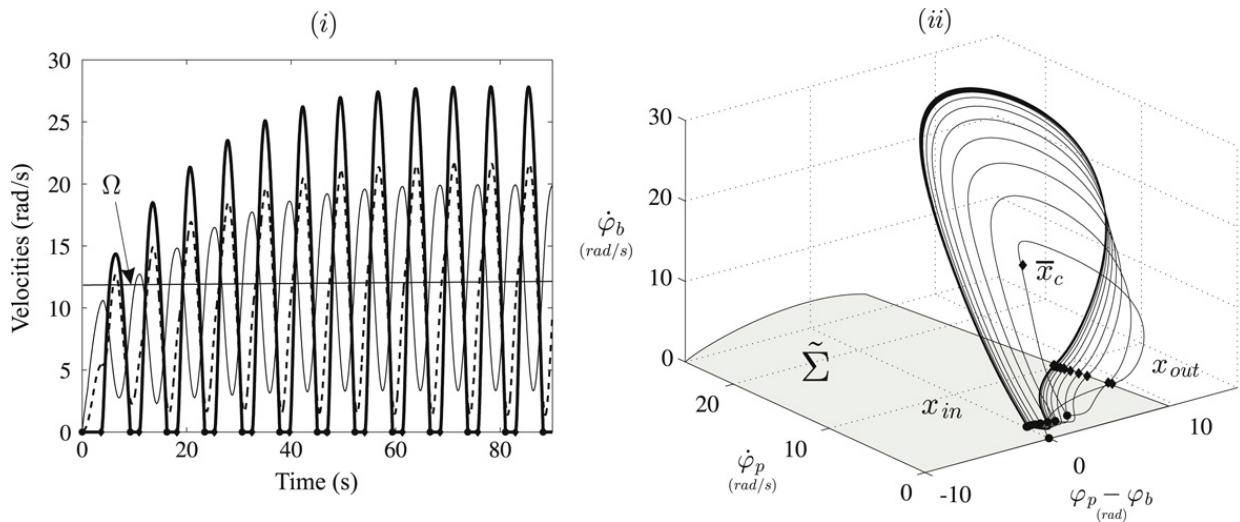
**Fig. 8.** Stick-slip oscillations may arise in the closed-loop system: (i) angular velocities, (ii) projection of the system trajectory in the phase space. $K_1 = 15$, $K_2 = 20$, $K_3 = 600$, $W_{ob} = 74\,386$ N, $\Omega = 12$ rad/s.
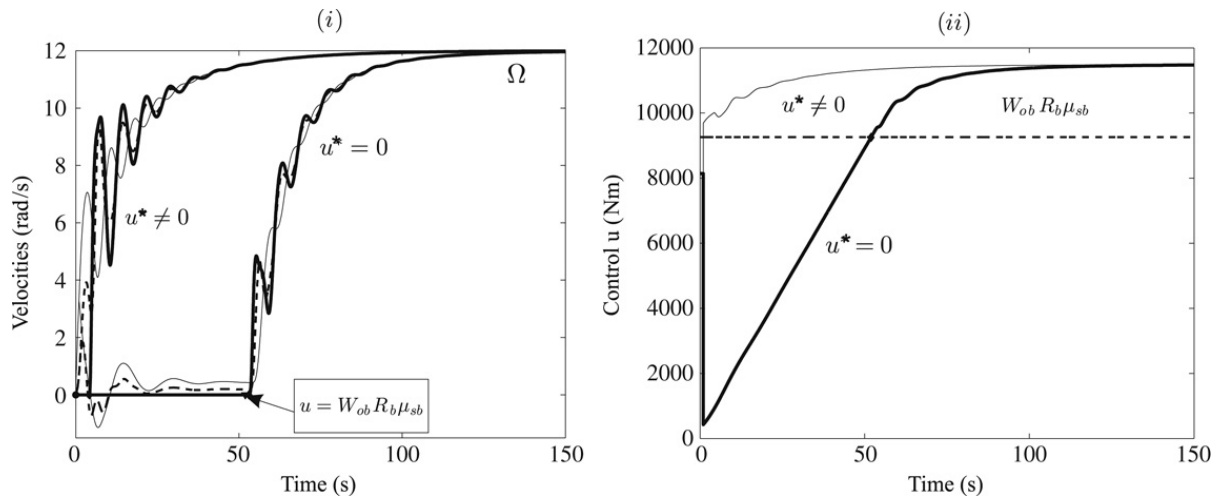


**Fig. 9.** The control goal is achieved: (i) velocities, (ii) control $u$. $K_1 = 15$, $K_2 = 20$, $K_3 = 30$, $W_{ob} = 74\,386$ N, $\Omega = 12$ rad/s.

with $b_i$, $i = 0, \ldots, 5$, depending on physical parameters, $K_1, K_2, K_3, \Omega$ and $W_{ob}$. The local asymptotic stability of $\bar{\mathbf{x}}_c$ can be ensured by means of the Liénard–Chipart criterion [29], i.e., when:

$$b_0 > 0, \ b_1 > 0, \ b_3 > 0, \ b_5 > 0, \ \Delta_3 = b_3(b_1b_2 - b_0b_3) + b_1(b_0b_5 - b_1b_4) > 0, \ \Delta_5 > 0, \tag{33}$$

with $\Delta_5$ the Hurwitz determinant of 5th order. The goal is choosing the controller parameters $K_1, K_2, K_3, \Omega$ and $W_{ob}$ so that stability conditions (33) are met.

In the first place, $K_1 > 0$ is established. The value of $K_1$ influences the transient system response, however, it does not significantly influence the stability properties of $\bar{\mathbf{x}}_c$. The higher $K_1$ is, the higher the overshooting in the velocities is, that is why it is convenient to maintain $K_1$ low enough. A convenient value of $K_1$ for the closed-loop system (28) and typical system parameters as in (11) is $K_1 = 15$. Low values of $K_2$ are also convenient for the transient system response not to be too oscillating. Now, $K_3$ will be selected.

An estimation of safe $\Omega$ and $W_{ob}$ can be obtained by evaluating conditions (33). Due to the high order of the system, the condition $\Delta_5 > 0$ is evaluated numerically. See the graphics in Fig. 10.(i). Parameters (11) and fixed $K_i$ are used. The wide-lined region is the region where conditions (33) are met. The curve corresponding to $b_1 = 0$, $b_3 = 0$, $b_1b_2 - b_0b_3 = 0$, $b_0b_5 - b_1b_4 = 0$ delimits this safe-parameter region. It can be noticed that for the cases in which $\bar{\mathbf{x}}_c$ is stable, this curve is the safe-region limit in spite of $K_1, K_2$ and $K_3$ variations (provided that $K_3$ is maintained low enough). The importance of the controller parameter $K_3$ can be appreciated from Fig. 10.(ii). Here, it can be seen that the higher $K_3$ is, the more reduced the safe-parameter region is, and the higher values of $\Omega$ are needed so that $\bar{\mathbf{x}}_c$ can be asymptotically stable.

These statements get clearer when looking at the bifurcation diagrams depicted in Fig. 11, obtained for a fixed $K_1 = 15$ and parameters (11). From these bifurcations diagrams, the conclusions achieved through the examination of conditions (33) are supported. Fig. 11.(i) depicts the variation of the steady velocity with respect to $\Omega$, for fixed $W_{ob} = 74\,386$ N, $K_2 = 10$, $K_3 = 300$. Two Hopf bifurcations appear, they give rise to two branches of unstable periodic orbits. These Hopf bifurcations
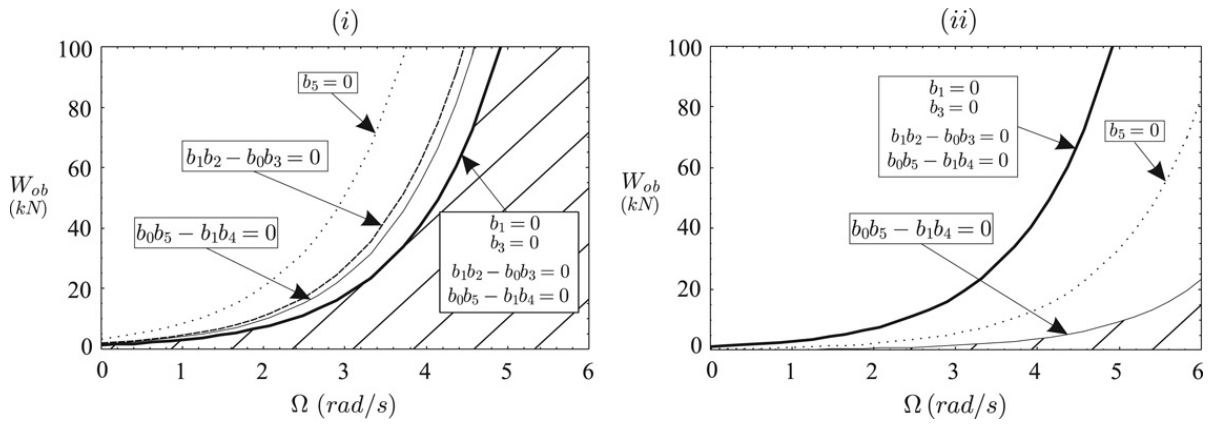
**Fig. 10.** Local stability of $\bar{\mathbf{x}}$, $(\Omega, W_{ob})$ for which some of the conditions (33) are satisfied: (i) $K_1 = 15$, $K_2 = 20$, $K_3 = 30$, (ii) $K_1 = 15$, $K_2 = 20$, $K_3 = 600$. The wide-lined region corresponds to parameter values for which the stability conditions (33) are met.
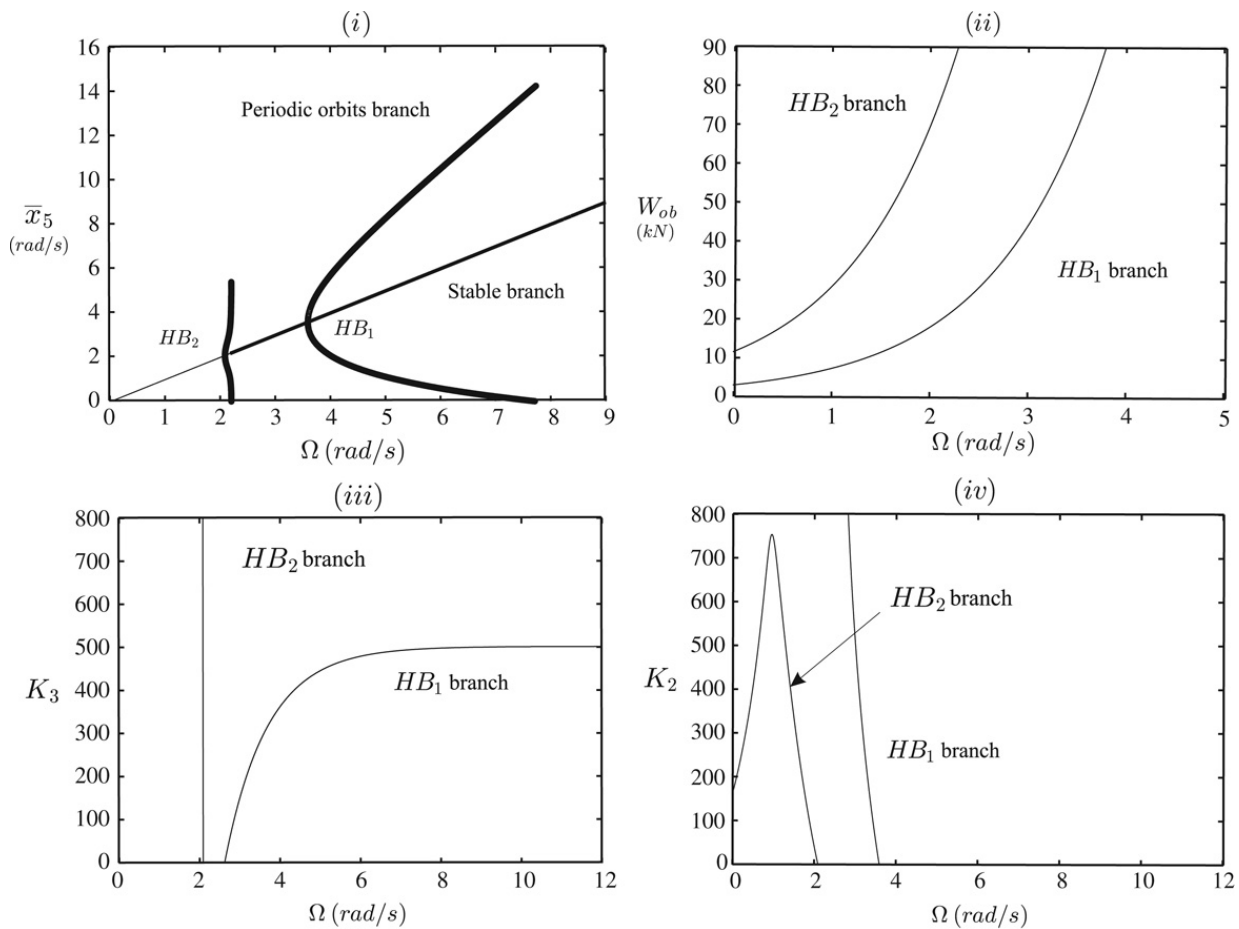


**Fig. 11.** Bifurcation diagrams for system (28) for parameters $\Omega$, $W_{ob}$, $K_2$ and $K_3$. Graphics have been obtained with XPPAUT [31].

points vary as long as $W_{ob}$, $K_2$ and $K_3$ vary, and different sets of periodic orbits can be obtained. The two Hopf-bifurcation branches for varying $(\Omega, W_{ob})$ with fixed $K_3$, $K_2$, for varying $(\Omega, K_3)$ with fixed $W_{ob}$, $K_2$, and for varying $(\Omega, K_2)$ with fixed $W_{ob}$, $K_3$ are depicted in Fig. 11.(ii), 11.(iii) and 11.(iv), respectively.

To conclude with, in order to achieve the control goal of driving the rotary velocities of drillstring components to a constant positive value, it is necessary that:

- $\Omega$ is high enough. See Figs. 10 and 11.(i) and 11.(ii). For typical drilling operation values of $\Omega$, $10 \le \Omega \le 14$ rad/s, we will be in the safe-parameter region for appropriate $K_i$ values.
- For high enough values of $\Omega$, the parameter $W_{ob}$ must be low enough. See Figs. 10 and 11.(ii).
- With independence of the value of the other parameters, $K_3$ must be low enough, $K_3 < K_3^*$. This is clearly appreciated on Fig. 11.(iii). A branch of Hopf bifurcation points giving rise to nondesired periodic orbits is present for all the values

of $\Omega$ and a fixed value of $K_3$. For parameters (11), this value is $K_3 = 503$. $K_3$ around this value must be avoided. For the example, by means of extensive simulations, it is concluded that the control goal is achieved with $K_3 < K_3^* = 385$.

- With high enough values of $\Omega$, the parameter $K_2$ is not a problem (Fig. 11.(iv)).

## 5. Conclusions

A 3-degree-of-freedom piecewise-smooth system modelling a conventional vertical oilwell drillstring has been proposed. An alternative method to describe bit-sticking phenomena in such a system has been presented. It is based on the characteristics of the system sliding motion and the equilibria. The sliding motion is due to the dry friction considered which models the bit-rock contact. Moreover, a linear state feedback control has been used to eliminate stick-slip oscillations. In the closed-loop system, the rotary velocities are driven to a desired value despite the presence of the sliding motion. The controller parameter design is made by analysing the bifurcations and transitions present at the system.

The analysis proposed can be successfully applied to other mechanical systems with multiple degrees of freedom exhibiting stick-slip oscillations and dry friction.

## Acknowledgements

## References

[1] J. Álvarez, E. Curiel, F. Verduzco, Complex dynamics in classical control systems, Systems Control Lett. 31 (1997) 277–285.
[2] M.F. Pérez Polo, M. Pérez Molina, Regular self-oscillating and chaotic behaviour of a PID controlled gimbal suspension gyro, Chaos Solitons Fractals 21 (2004) 1057–1074.
[3] G. Luo, L. Ma, X. Lv, Dynamic analysis and suppressing chaotic impacts of a two-degree-of-freedom oscillator with a clearance, Nonlinear Anal. RWA (2007) doi:10.1016/j.nonrwa.2007.11.002.
[4] S.W. Shaw, On the dynamic response of a system with dry friction, J. Sound Vib. 108 (2) (1986) 305–325.
[5] P. Stelter, W. Sextro, Bifurcations in dynamic systems with dry friction, Internat. Ser. Numer. Math. 97 (1991) 343–347.
[6] H. Dankowicz, A.B. Nordmark, On the origin and bifurcations of stick-slip oscillations, Phys. D 136 (2000) 280–302.
[7] R.I. Leine, D.H. van Campen, B.L. van de Vrande, Bifurcations in nonlinear discontinuous systems, Nonlinear Dynam. 23 (2) (2000) 105–164.
[8] U. Galvanetto, Some discontinuous bifurcations in a two-block stick-slip system, J. Sound Vib. 248 (4) (2001) 653–669.
[9] A.C.J. Luo, B.C. Gegg, Stick and non-stick periodic motions in periodically forced oscillators with dry friction, J. Sound Vib. 291 (2006) 132–168.
[10] E.M. Navarro-López, D. Cortés, Avoiding harmful oscillations in a drillstring through dynamical analysis, J. Sound Vib. 307 (1–2) (2007) 152–171.
[11] G.W. Halsey, Å Kyllingstad, A. Kylling, Torque feedback used to cure slip-stick motion, in: 63rd SPE Annual Tech. Conf. and Exhibition, 1988, pp. 277–282.
[12] Y.-Q. Lin, Y.-H. Wang, Stick-slip vibration of drill strings, J. Engrg. Industry 113 (1991) 38–43.
[13] J.F. Brett, The genesis of torsional drillstring vibrations, SPE Drilling Eng. (September) (1992) 168–174.
[14] J.D. Jansen, L. van den Steen, Active damping of self-excited torsional vibrations in oil well drillstrings, J. Sound Vib. 179 (4) (1995) 647–668.
[15] F. Abbassian, V.A. Dunayevsky, Application of stability approach to torsional and lateral bit dynamics, SPE Drilling Completion 13 (2) (1998) 99–107.
[16] A.F.A. Serrarens, M.J.G. van de Molengraft, J.J. Kok, L. van den Steen, $H_\infty$ control for suppressing stick-slip in oil well drillstrings, IEEE Control Syst. (April) (1998) 19–30.
[17] A.S. Yigit, A.P. Christoforou, Coupled torsional and bending vibrations of actively controlled drillstrings, J. Sound Vib. 234 (1) (2000) 67–83.
[18] N. Mihajlović, A.A. van Veggel, N. van de Wouw, H. Nijmeijer, Analysis of friction-induced limit cycling in an experimental drill-string system, ASME J. Dynam. Systems Measurement Control 126 (2004) 709–720.
[19] E.M. Navarro-López, R. Suárez-Cortez, Vibraciones mecánicas en una sarta de perforación: Problemas de control, Rev. Ib. de Automática e Informática Industrial 2 (1) (2005) 43–54.
[20] P. Sananikone, O. Kamoshima, D.B. White, A field method for controlling drillstring torsional vibrations, in: IADC/SPE Drilling Conference, New Orleans, 1992 pp. 443–452.
[21] D.R. Pavone, J.P. Desplans, Application of high sampling rate downhole measurements for analysis and cure of stick-slip in drilling, in: SPE Annual Technical Conference and Exhibition, New Orleans, 1994 pp. 335–345.
[22] E.M. Navarro-López, R. Suárez-Cortez, Practical approach to modelling and controlling stick-slip oscillations in oilwell drillstrings, in: IEEE International Conference on Control Applications, Taipei, Taiwan, 2004, pp. 1454–1460.
[23] E.M. Navarro-López, D. Cortés, Controller parameters selection through bifurcation analysis in a piecewise-smooth system, in: HSCC, in: Lecture Notes in Comput. Sci., vol. 4416, Springer-Verlag, Berlin, 2007, pp. 736–740.
[24] Tri-cone manual de barrenas. USA: Hughes Tool Company, 1982.
[25] Y.A. Kuznetsov, S. Rinaldi, A. Gragnani, One-parameter bifurcations in planar Filippov systems, Internat. J. Bifur. Chaos 13 (8) (2003) 2157–2188.
[26] V.I. Utkin, Sliding Modes in Control Optimization, Springer-Verlag, Berlin, 1992.
[27] A.F. Filippov, Differential Equations with Discontinuous Right-hand Sides, Kluwer Academic Publishers, Dordrecht, 1988.
[28] J.P. LaSalle, The Stability of Dynamical Systems, Society for Industrial and Applied Mathematics, Hamilton Press, 1976.
[29] A. Liénard, M.H. Chipart, Sur la signe de la partie reelle des racines d'une équation algebrique, J. Math. Pures Appl. 10 (1914) 291–346.
[30] W.M. Liu, Criterion of Hopf bifurcations without using eigenvalues, J. Math. Anal. Appl. 182 (1994) 250–256.
[31] B. Ermentrout, Simulating, Analyzing, and Animating Dynamical Systems (A Guide to XPPAUT for Researchers and Students), SIAM Software Environments Tools, 2002.